Dynamic switching of 1.9 A /1.76 kV Forward Current NiO/β-Ga_2O_3 Rectifiers

Jian-Sian Li[1], Chao-Ching Chiang[1], Xinyi Xia[1], Cheng-Tse Tsai[2], Fan Ren[1], Yu-Te Liao[2] and S.J. Pearton[3]

[1] Department of Chemical Engineering, University of Florida, Gainesville, FL 32606 USA

[2] Department of Electronics and Electrical Engineering, National Yang Ming Chiao Tung University, Hsinchu 30010, Taiwan

[2] Department of Materials Science and Engineering, University of Florida, Gainesville, FL 32606 USA

Abstract

The switching performance of vertical geometry NiO/β-Ga_2O_3 rectifiers with a reverse breakdown voltage of 1.76 kV (0.1 cm diameter, 7.85 x10^{-3} cm^2 area) and an absolute forward current of 1.9 A fabricated on 20 μm thick epitaxial β-Ga_2O_3 drift layers and a double layer of NiO to optimize breakdown and contact resistance was measured with an inductive load test circuit. The Baliga figure-of-merit of the devices was 175 MW.cm^{-2}, with on-state resistance of 17.8 mΩ.cm^2. The recovery characteristics for these rectifiers switching from forward current of 1 A to reverse off-state voltage of -550 V showed a recovery time (t_{rr}) of 101 ns, with a peak current value of 1.4A for switching from 640V. There was no significant dependence of t_{rr} on switching voltage or forward current.

Introduction

Wide and ultra-wide bandgap semiconductors are attracting a lot of interest for next generation power electronics applications because of their advantages in terms of lower on-state resistances and higher power levels [1-6]. More robust power electronics that withstand higher operating temperatures, a smaller form factor, and higher efficiency will significantly improve the reliability and security of power grids [1-5], especially with all the switching needed to incorporate generation from renewable sources. In addition, they are more radiation-hard than conventional Si, so with the increasing number of satellites in low Earth orbit (LEO), there is a high demand for space-based radiation-hardened components capable of withstanding high radiation effects caused due to solar flares [2-6]. The growth in global radiation-hardened electronics for space applications market is expected to be driven by increasing demand for communication and Earth observation satellites [2-6]. In addition, there is an evolution from hydro-pneumatic to more electrical disposition of power in aircraft [5], leading to the need for reliable power electronic components in current and future aerospace applications.

While SiC and GaN are already commercialized for power switching systems with improved power density and efficiency [1-7], there is interest in the ultra-wide bandgap semiconductor Ga_2O_3 [7-13], especially the stable polytype, monoclinic β-Ga_2O_3 [7,8,10], both as unipolar Schottky rectifiers and with p-n heterojunctions with other oxides [14-47]. Recently, lateral β-Ga_2O_3 transistors with breakdown voltage 8 kV have been reported [14]. There is even more potential in vertical geometry devices, with a recent report of 6kV breakdown in a device with SiO_2 edge termination [48]. One drawback of β-Ga_2O_3 is the absence of a practical p-type doping capability. This has spurred interest in use of p-type NiO for vertical p–n heterojunction power diodes with Ga_2O_3 [17-46, 49, 50, 51], although there are few reports of switching characteristics of such devices [52]. Sputtered NiO_x is a well-developed system, producing polycrystalline layers (bandgap ~ 3.7–4.0 eV, mobility < 1 cm^2V^{-1} s^{-1} and hole concentrations in the 10^{18}-10^{19} cm^{-3} range) [49]. There have been a range of impressive device demonstrations with NiO/β-Ga_2O_3 rectifiers, including a Baliga's figure of merit of 5.18 GW.cm $^{-2}$ [50] and a static V_B of 4.7 kV [53]. For large area devices, a NiO/Ga_2O_3 rectifier of 1 mm ^{2} area showed a forward current of 5A and breakdown voltage 700 V [24], while Gong et al.[38] reported a 1.37 kV/12 A NiO/β-Ga_2O_3 heterojunction diode with ns reverse recovery and rugged surge-current capability. Hu et al.[54] reported small area 1.2 kV/2.9 mΩ·cm^2 vertical NiO/β-Ga_2O_3 diodes with a reverse recovery time (t_{rr}) of ~ 60 ns and reverse recovery charge (Qrr) of ~ 1.97 nC, which is superior to a reference commercial Si fast-recovery diode.

In this paper, we report the voltage and current dependence of reverse recovery times of 1.9 A /1.76 kV NiO/Ga_2O_3 rectifiers fabricated on 20 μm epitaxial layers on bulk conducting substrates using an inductive load test circuit. These devices were switched from 1 A to -550 V with t_{rr} of 101 ns and no significant voltage or current dependence in the ranges investigated.

Experimental

The drift region of the material used to make the rectifiers consisted of a 20 μm thick, Si doped halide vapor phase epitaxy (HVPE) layer with carrier concentration $2x10^{16}$ cm^{-3}, grown on a (001) surface orientation Sn-doped β-Ga_2O_3 single crystal (Novel Crystal Technology, Japan). A full area Ti/Au backside Ohmic contact was formed by e-beam evaporation and annealed at 550̊C for 1minute under N_2 ambient [9,10,53]. NiO was deposited by magnetron sputtering at 3mTorr and 150W of 13.56 MHz power using two separate targets operated at the same time to double the deposition rate to around 0.2 Å.sec^{-1}. The Ar/O_2 ratio was used to control the doping in the NiO in the range $2x10^{18}$- 3 $x10^{19}$ cm^{-3}, with mobility < 1 cm^2 ·V^{-1} s^{-1}. A double NiO layer structure was used to optimize both breakdown voltage and contact resistance. A schematic of the final device structure is shown in Figure 1. A two-layer NiO structure with respective thicknesses of 10/10 nm and doping of 2.6 $x10^{19}/3.5x10^{18}$ cm^{-3} was used. The Ni/Au contact metal (1mm diameter) was deposited by electron beam evaporation onto the NiO layer after annealing at 300°C under O_2 ambient.

For dc characterization, the current-voltage (I-V) characteristics were recorded with a Tektronix 370-A curve tracer, 371-B curve tracer and Agilent 4156C was used for forward and reverse current measurements. The reverse breakdown voltage was defined as the bias for a reverse current reaching 0.1 $A.cm^2$, which has been standard for previous studies [(42,51)]. To measure the response of the diode's recovery time, a clamped inductive load test circuit was designed and fabricated for the switching measurement [(13)].

Results and Discussion

Figure 2 shows the single sweep forward I-V characteristics in log (a) and linear (b) form, along with the extracted on-state resistance of 17.8 $m\Omega cm^2$. The turn-on voltage was 1.7 V, consistent with literature values and higher than is typically obtained with conventional Ga_2O_3 Schottky rectifiers. The maximum forward current achieved was 1.9 A. The forward direction characteristic was dominated by the thermionic emission (TE) current [(8)].

The reverse I-V characteristics are shown in Figure 3(a) for the low-voltage range. In this region, the current is dominated by thermionic field emission (TFE), while at higher reverse voltages tunneling currents are also present [(8)]. Figure 3(b) shows that a maximum breakdown voltage value of ~1.76 kV was obtained, a record for large area NiO/Ga_2O_3 devices. This leads to a power figure-of-merit of 175 $MW.cm^{-2}$. By sharp contrast, a conventional Ni/Au/Ga_2O_3 Schottky rectifier of the same dimensions without edge termination fabricated on the same wafer but without the NiO had a reverse breakdown of only 498V, as also shown in Figure 3 (b). This demonstrates the effectiveness of the extension of the NiO in the structure in providing edge termination.

Figure 4 shows the diode on-off ratio for the NiO/ Ga_2O_3 devices when switching from -1V forward voltage to reverse voltages in the range was in the range 2.7×10^{10}-2.2×10^{8} over our measurement range up to 100V.

To measure the reverse recovery time of the rectifiers, τ_{rr}, defined as the time that taken for rectifiers recover to the current level of 25% of the reverse recovery current, I_{rr}. a clamped inductive load test circuit was designed and fabricated for the switching measurement, as shown schematically in Figure 5 (10,13). During the rectifier switching (top of Figure 5), a double pulse was employed to drive the Si transistor (STMicroelectronics STW9N150, 1.5 kV, 8A n-channel MOSFET), and the duration of the duty cycle used to adjust the Ga_2O_3 Schottky diode forward current (13). The inductor (J.W. Miller 1140–153K-RC, 15 mH), was initially charged from the DC power supply by turning on the transistor. Once this was turned off, the pre-charged inductor released charge through the forward-biased diode. Upon turning the transistor back on, the rectifier was switched from the on-state to the off- state, leading to charge depletion. Figure 5 also shows the operational waveforms of the switching circuit. Photographs of the measurement setup and the circuit board are shown in Figure 6. More details on this circuit design and operation have been published previously (13).

Figure 7 shows the switching node performance of a NiO/Ga_2O_3 rectifier. This device was switched from 1 A of forward current to a reverse off-stage voltage of -550 V. The circuit was operated with a period of 50µsec, duty cycle of 0.75 µsec (1.5%). The MOSFET pulse was 10V and the power supply for the rectifier was 800V. The recovery time was 101 ns with Irr of 0.62

A, and the dI/dt was calculated as 27.8 A/μs for I_F of 1A. The diode achieved 1A/550V switching, with a peak value of 1.4A/640V. The reverse recovery time was defined as the time that taken for rectifiers recover to the current level of 25% of I_{rr}. Since the rectifier itself has a recovery time of ~11 ns, we believe the additional recovery time measured from this system results from parasitics on the PCB board. The reverse recovery time did not show any significant dependence on either off state voltage or on-state current. This is a result of the short minority carrier lifetime of β-Ga_2O_3 (7,8,11). These results on large area rectifiers with high total current and an ability to operate in the > 1200V class range are another step in the advance of Ga_2O_3 for power rectification applications.

Summary and Conclusions

NiO/ β-Ga_2O_3 vertical Schottky rectifiers with an absolute forward current of 1.9 A and 1.76 kV breakdown voltage were demonstrated with large area (7.85×10^{-3} cm^2) on 20 μm thick drift layers. Conventional NiAu/Ga_2O_3 Schottky rectifiers of the same size fabricated on the same wafers had breakdown voltages of 498V. These devices were switched from 1 A to -550 V with trr of 101 ns and no significant voltage or current dependence in the ranges investigated. These results show the potential of p-n heterojunction NiO/Ga_2O_3 vertical Schottky rectifiers in high power device and high-speed switching technologies.

Acknowledgments

The work at UF was performed as part of Interaction of Ionizing Radiation with Matter University Research Alliance (IIRM-URA*)*, sponsored by the Department of the Defense, Defense Threat Reduction Agency under award HDTRA1-20-2-0002. The content of the information does not necessarily reflect the position or the policy of the federal government, and no official endorsement should be inferred. The work at UF was also supported by NSF DMR

1856662 (James Edgar). The authors at National Yang Ming Chiao Tung University, Hsinchu 30010, Taiwan would like to thank the Ministry of Science and Technology, Taiwan, for their financial support under the grants MOST 107-2918-I-009-010 and 111-2628-E-A49-013.

Data Availability

The data that supports the findings of this study are available within the article and its supplementary material.

Declarations

The authors have no conflicts to disclose

References

1. H. Fu, K. Fu, S. Chowdhury, T. Palacios and Y. Zhao, IEEE Trans Electron Dev, 68, 3212 (2021)

2. G. Deboy, O. Haeberlen, and M. Treu, CPSS Trans. Power Electron. Applicat., 2, 89 (2017).

3. Y. Zhang and T. Palacios, IEEE Trans Electron Dev, 67, 3960 (2020).

4. J. Ballestín-Fuertes, J. Muñoz-Cruzado-Alba, J. F. Sanz-Osorio and E. Laporta-Puyal, Electronics, 10, 677 (2021).

5. A.J. Wileman, Sohaib Aslam, Suresh Perinpanayagam, Prog Aerospace Sci, 127, 100739 (2021).

6. Matteo Meneghini, Carlo De Santi, Idriss Abid, Matteo Buffolo, Marcello Cioni, Riyaz Abdul Khadar, Luca Nela, Nicolò Zagni, Alessandro Chini, Farid Medjdoub, Gaudenzio Meneghesso, Giovanni Verzellesi, Enrico Zanoni and Elison Matioli, J. Appl. Phys.130, 181101 (2021).

7. M. H. Wong and M. Higashiwaki, IEEE Trans Electron Dev, 67, 3925 (2020).

8. Andrew J. Green, James Speck, Grace Xing, Peter Moens, Fredrik Allerstam, Krister Gumaelius, Thomas Neyer, Andrea Arias-Purdue, Vivek Mehrotra, Akito Kuramata, Kohei Sasaki, Shinya Watanabe, Kimiyoshi Koshi, John Blevins, Oliver Bierwagen, Sriram Krishnamoorthy, Kevin Leedy, Aaron R. Arehart, Adam T. Neal, Shin Mou, Steven A. Ringel, Avinash Kumar, Ankit Sharma, Krishnendu Ghosh, Uttam Singisetti, Wenshen Li, Kelson Chabak, Kyle Liddy, Ahmad Islam, Siddharth Rajan, Samuel Graham, Sukwon Choi, Zhe Cheng, and Masataka Higashiwaki, APL Mater. 10, 029201 (2022).

9. J. Yang, F. Ren, M. Tadjer, S. J. Pearton, and A. Kuramata, ECS J. Solid State Sci. Technol, 7, 92 (2017).

10. J. Yang, F. Ren, Y. Chen, Y. Liao, C. Chang, J. Lin, Marko J. Tadjer, S. J. Pearton and Akito Kuramata, IEEE J. Electron Devices Soc, 7, 57 (2019).

11. S. J. Pearton, Fan Ren, Marko Tadjer and Jihyun Kim, J. Appl. Phys. 124, 220901 (2018).

12. Chenlu Wang, Jincheng Zhang, Shengrui Xu, Chunfu Zhang, Qian Feng, Yachao Zhang, Jing Ning, Shenglei Zhao, Hong Zhou and Yue Hao, J. Phys. D: Appl. Phys. 54, 243001 (2021).

13. Yen-Ting Chen, Jiancheng Yang, Fan Ren, Chin-Wei Chang, Jenshan Lin, S. J. Pearton, Marko J. Tadjer, Akito Kuramata and Yu-Te Liao, ECS J. Solid State Sci. Technol. 8, Q3229 (2019).

14. S. Sharma, K. Zeng, S. Saha, U. Singisetti, IEEE Electron Dev. Lett. 41, 6 836 (2020).

15. Jiancheng Yang, F. Ren, Marko Tadjer, S. J. Pearton and A. Kuramata, AIP Adv. 8, 055026 (2018).

16. S. Roy, A. Bhattacharyya, P. Ranga, H. Splawn, J. Leach and S. Krishnamoorthy, IEEE Electron Dev. Lett. 42, 1140 (2021).

17. X. Lu, X. Zhou, H. Jiang, K. W. Ng, Z. Chen, Y. Pei, K. M. Lau, and G. Wang, IEEE Electron Dev Lett. 41, 449 (2020).

18. B. Chatterjee, K. Zeng, C. D. Nordquist, U. Singisetti and S. Choi, IEEE Trans. Compon, Packaging Man Technol, 9, 2352 (2019).

19. K. D. Chabak, K. D. Leedy, A. J. Green, S. Mou, A. T Neal, T. Asel, E. R. Heller, N. S. Hendricks, K. Liddy, A. Crespo, N. C. Miller, M. T. Lindquist, N. Moser, R. C. Fitch Jr, D. E. Walker Jr, D. L Dorsey and G. H. Jessen, Semicond Sci Technol, 35, 013002 (2020).

20. Zongyang Hu, Kazuki Nomoto, Wenshen Li, Zexuan Zhang, Nicholas Tanen, Quang Tu Thieu, Kohei Sasaki, Akito Kuramata, Tohru Nakamura, Debdeep Jena, and Huili Grace Xing, Appl. Phys. Lett. 113, 122103 (2018).

21. W. Li, K. Nomoto, Z. Hu, D. Jena and H. G. Xing, IEEE Electron Dev. Lett, 41, 107 (2020).

22. Ribhu Sharma, Minghan Xian, Chaker Fares, Mark E. Law, Marko Tadjer, Karl D. Hobart, Fan Ren and Stephen J. Pearton, J. Vac. Sci. Technol A 39, 013406 (2021).

23. Wenshen Li, Devansh Saraswat, Yaoyao Long, Kazuki Nomoto, Debdeep Jena, and Huili Grace Xing, Appl. Phys. Lett. 116, 192101 (2020)

24. Y. Lv, Y. Wang, X. Fu , Shaobo Dun, Z. Sun, Hongyu Liu, X. Zhou, X. Song, K. Dang, S. Liang, J. Zhang, H. Zhou, Z. Feng, S. Cai and Yue Hao, IEEE Trans Power Electron. 36, 6179 (2021).

25. Jiancheng Yang, Minghan Xian, Patrick Carey, Chaker Fares, Jessica Partain, Fan Ren, Marko Tadjer, Elaf Anber, Dan Foley, Andrew Lang, James Hart, James Nathaniel, Mitra L. Taheri, S. J. Pearton and Akito Kuramata, Appl. Phys. Lett. 114, 232106 (2019)

26. Z. Jian, S. Mohanty, and E. Ahmadi,Appl. Phys. Lett., 116, 152104 (2020).

27. T. Harada, and A. Tsukazaki, Appl. Phys. Lett., 116, 232104 (2020).

28. C. -H. Lin, Y. Yuda, M. H. Wong, M. Sato, N. Takekawa, K. Konishi, T. Watahiki, M. Yamamuka, H. Murakami, Y. Kumagai and Masataka Higashiwaki, IEEE Electron Dev. Lett., 40, 1487 (2019).

29. W. Xiong, X. Zhou, G. Xu, Q. He, G. Jian, C. Chen, Y. Yu, W. Hao, X. Xiang, X. Zhao, W. Mu, Z. Jia, X. Tao, and S. Long, IEEE Electron. Dev. Lett.42, 430 (2021).

30. S. J. Pearton, J. Yang, P. H. Cary, F. Ren, J. Kim, M. J. Tadjer and M. A. Mastro,Appl. Phys. Rev., 5, 011301 (2018).

31. Ming Xiao, Boyan Wang , Jingcun Liu , Ruizhe Zhang, Zichen Zhang, Chao Ding, Shengchang Lu, Kohei Sasaki, Guo-Quan Lu, Cyril Buttay, and Yuhao Zhang, IEEE Trans. Power Electron. 36, 8565 (2021).

32. Arkka Bhattacharyya, Shivam Sharma, Fikadu Alema, Saurav Roy, Carl Peterson, George Seryogin, Andrei Osinsky, Uttam Singisetti, Sriram Krishnamoorthy, Appl. Phys. Expr (in press, 2022)

33. X. Lu, Xianda Zhou, Huaxing Jiang, Kar Wei Ng, Zimin Chen, Yanli Pei, Kei May Lau and Gang Wang, IEEE Electron Dev. Lett.41, 449 (2020).

34. Chenlu Wang, Hehe Gong, Weina Lei, Y. Cai, Z. Hu, Shengrui Xu, Zhihong Liu , Qian Feng , Hong Zhou, Jiandong Ye, Jincheng Zhang, Rong Zhang, and Yue Hao, IEEE Electron Dev. Lett, 42, 485 (2021).

35. S. Roy, A. Bhattacharyya, P. Ranga, H. Splawn, J. Leach, and S. Krishnamoorthy, IEEE Electron Device Lett., 42, 1540 (2021).

36. Qinglong Yan, Hehe Gong, Jincheng Zhang, Jiandong Ye, Hong Zhou, Zhihong Liu, Shengrui Xu, Chenlu Wang, Zhuangzhuang Hu, Qian Feng, Jing Ning, Chunfu Zhang, Peijun Ma, Rong Zhang, and Yue Hao, Appl. Phys. Lett. 118, 122102 (2021).

37. H. H. Gong, X. H. Chen, Y. Xu, F.-F. Ren, S. L. Gu and J. D. Ye, Appl. Phys. Lett., 117, 022104 (2020).

38. Hehe Gong, Feng Zhou, Weizong Xu , Xinxin Yu, Yang Xu, Yi Yang, Fang-fang Ren, Shulin Gu, Youdou Zheng, Rong Zhang, Hai Lu and Jiandong Ye, IEEE Trans. Power Electron., 36, 12213 (2021).

39. H. H. Gong, X. X. Yu, Y. Xu, X. H. Chen, Y. Kuang, Y. J. Lv, Y. Yang, F.-F. Ren, Z. H. Feng, S. L. Gu, Y. D. Zheng, R. Zhang, and J. D. Ye , Appl. Phys. Lett. 118, 202102 (2021)

40. H. H. Gong, X. H. Chen, Y. Xu, Y. T. Chen, F. F. Ren, B. Liu, S. L. Gu, R. Zhang, and J. D. Ye, IEEE Trans. Electron Dev. 67, 3341 (2020).

41. W. Hao, Q. He, K. Zhou, G. Xu, W. Xiong, X. Zhou, G. Jian, C. Chen, X. Zhao, and S. Long, Appl. Phys. Lett., 118, 043501 (2021).

42. F. Zhou, Hehe Gong, Weizong Xu, Xinxin Yu, Yang Xu, Yi Yang, Fang-fang Ren, Shulin Gu, Youdou Zheng, Rong Zhang, Jiandong Ye and Hai Lu, IEEE Trans. Power Electron, 37, 1223 (2022)

43. Qinglong Yan, Hehe Gong, Jincheng Zhang, Jiandong Ye, Hong Zhou, Zhihong Liu, Shengrui Xu, Chenlu Wang, Zhuangzhuang Hu, Qian Feng, Jing Ning, Chunfu Zhang, Peijun Ma, Rong Zhang, and Yue Hao, Appl. Phys. Lett. 118, 122102 (2021).

44. Qinglong Yan, Hehe Gong, Hong Zhou, Jincheng Zhang, Jiandong Ye, Zhihong Liu, Chenlu Wang, Xuefeng Zheng, Rong Zhang, and Yue Hao, Appl. Phys. Lett. 120, 092106 (2022).

45. Y. J. Lv, Y. G. Wang, X. C. Fu, S. B. Dun, Z. F. Sun, H. Y. Liu, X. Y. Zhou, X. B. Song, K. Dang, S. X. Liang, J. C. Zhang, H. Zhou, Z. H. Feng, S. J. Cai, and Y. Hao, IEEE Trans. Power Electron. 36, 6179 (2021).

46. Jiaye Zhang, Shaobo Han, Meiyan Cui, Xiangyu Xu, Weiwei Li, Haiwan Xu, Cai Jin, Meng Gu, Lang Chen and Kelvin H. L. Zhang, ACS Appl. Electron. Mater. 2, 456 (2020).

47. Jiancheng Yang, Fan Ren, Marko Tadjer, S.J. Pearton and A Kuramata, ECS J. Solid State Sci. Technol.7, Q92 (2018).

48. Pengfei Dong, Jincheng Zhang, Qinglong Yan, Zhihong Liu, Peijun Ma, Hong Zhou, and Yue Hao, IEEE Electron. Dev. Lett. (in press, 2022).

49. J.A. Spencer, A.L. Mock, A.G. Jacobs, M. Schubert, Y. Zhang and M.J. Tadjer, Appl. Phys. Rev. 9, 011315 (2022).

50. Yuangang Wang, Hehe Gong, Yuanjie Lv , Xingchang Fu, Shaobo Dun, Tingting Han, Hongyu Liu, Xingye Zhou, Shixiong Liang, Jiandong Ye, Rong Zhang, Aimin Bu, Shujun Cai and Zhihong Feng, IEEE Trans. Power Electron. 37, 3743 (2022).

51. Hong Zhou, Shifan Zeng, Jincheng Zhang, Zhihong Liu, Qian Feng, Shengrui Xu, Jinfeng Zhang and Yue Hao, Crystals 11, 1186 (2021).

52. A. Takatsuka, K. Sasaki, D. Wakimoto, Q. T. Yhieu, Y. Koishikawa, J.Arima, J. Hirabayashi, D. Inokuchi, Y. Fukumitsu, A. Kuramata, S. Yamakoshi, "Fast Recovery Performance of β-Ga_2O_3 Trench MOS Schottky Barrier Diodes", in Proc. of the 76th Device Research Conf., IEEE, pp. 1–2, USA 2018.

53. Jian-Sian Li, Chao-Ching Chiang, Xinyi Xia, Timothy Jinsoo Yoo, Fan Ren, Honggyu Kim and S.J. Pearton, Appl. Phys. Lett (in press).

54. Yawei Hu, Shanyong Wang, Ziqi Yang, Rongsheng Chen, Xing Lu, Yuan Ren, Xianda Zhou, Zimin Chen, Yanli Pei, Gang Wang, Proceedings of the 2020 32nd International Symposium on Power Semiconductor Devices and ICs (ISPSD) September 13 – 18, 2020, Vienna, Austria

Figure Captions

Figure 1. Schematic cross-section view of the double layer NiO/Ga_2O_3 heterojunction rectifier structure.

Figure 2. (a) Forward current-voltage characteristic and R_{ON} values (b) Linear plot of forward I-V characteristic.

Figure 3. (a) Reverse I-V characteristic in low voltage range (b). Reverse I-V characteristics showing comparison of breakdown voltages of NiO/Ga_2O_3 heterojunction rectifier to that of a standard Schottky rectifier of the same size fabricated on the same wafer. The arrows mark where breakdown occurs, to guide the eye. This is slightly different than the definition used to standardize V_B.

Figure 4. On-off ratio of double NiO layer NiO/Ga_2O_3 heterojunction rectifiers in which the bais was switched from -5V forward to the voltage shown on the x-axis.

Figure 5. Schematic of switching circuitry and voltage/current waveforms of the circuit operations.

Figure 6. (a) Measurement set-up and (b) circuit board of the switching circuitry for measuring the dynamic switching characteristics of the NiO/Ga_2O_3 rectifiers.

Figure 7. Switching waveform for NiO/Ga_2O_3 rectifiers for voltage period of 50 uS, duty cycle of 0.75 uS (1.5%), power Supply voltage of 800 V. The extracted switching results were t_{rr} = 101 nS, I_{rr} = -0.62 Aa and dI/dt = 27.8 A/μs for I_F = 1 A. The diode achieved 1A/550V switching, with a peak value of 1.4A/640V.

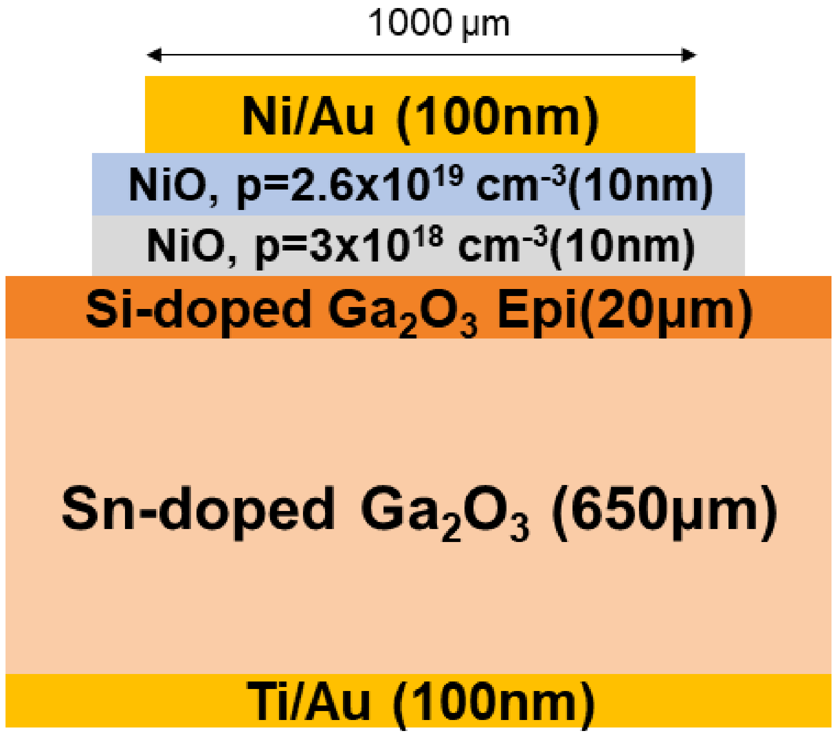
1000 µm
Ni/Au (100nm)
NiO, p=2.6x10^19 cm^-3(10nm)
NiO, p=3x10^18 cm^-3(10nm)
Si-doped Ga2O3 Epi(20µm)
Sn-doped Ga2O3 (650µm)
Ti/Au (100nm)

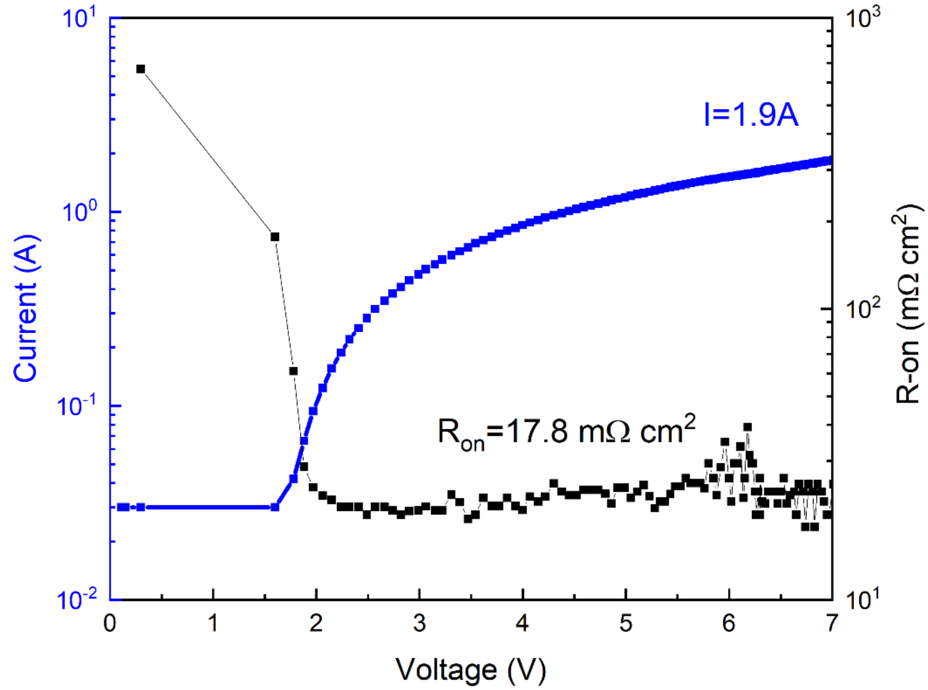

Current (A)
R-on (mΩ cm²)
I=1.9A
R_on=17.8 mΩ cm²
Voltage (V)

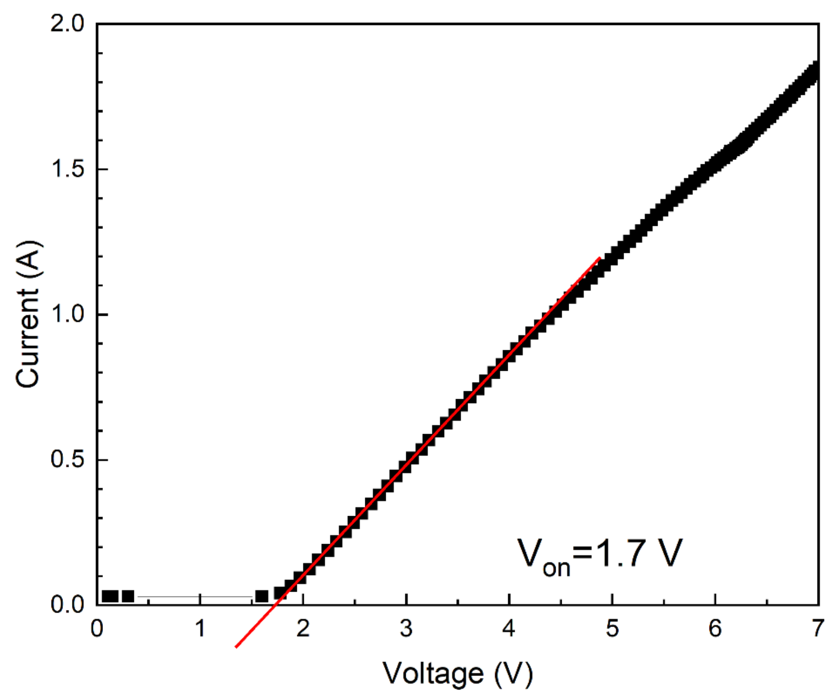

Current (A)
V_on=1.7 V
Voltage (V)

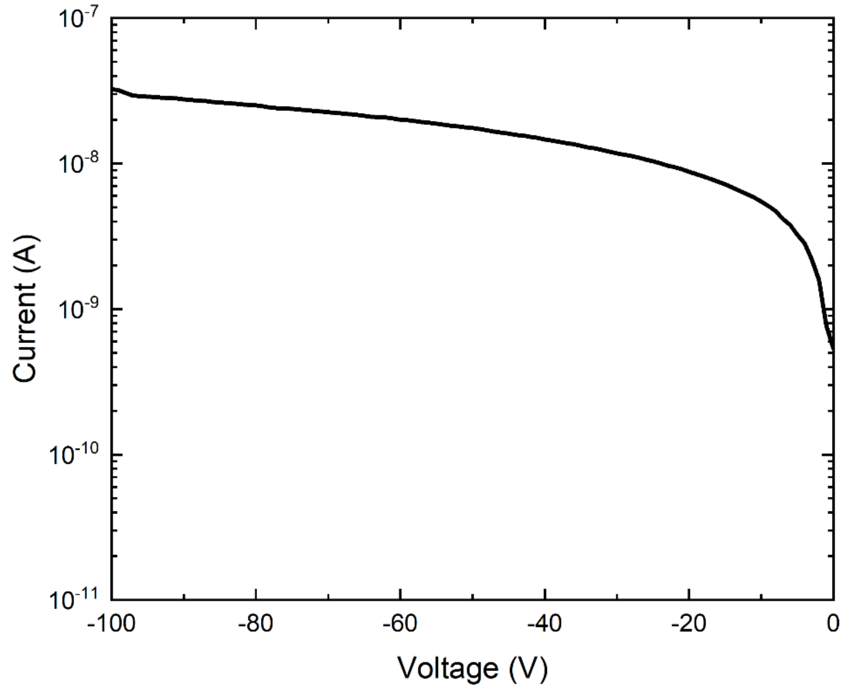

Current (A)
Voltage (V)

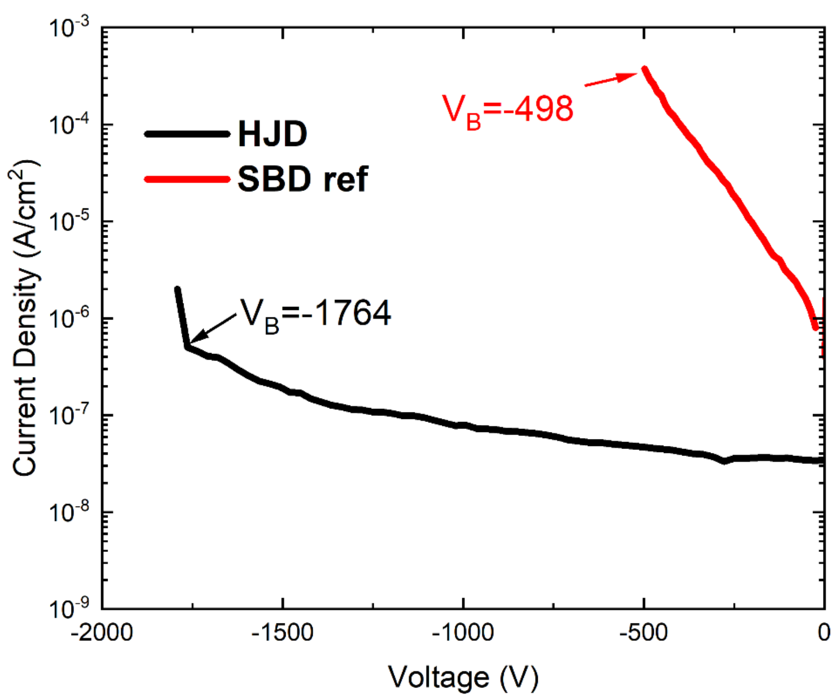

HJD
SBD ref
V_B=-498
V_B=-1764
Current Density (A/cm²)
Voltage (V)

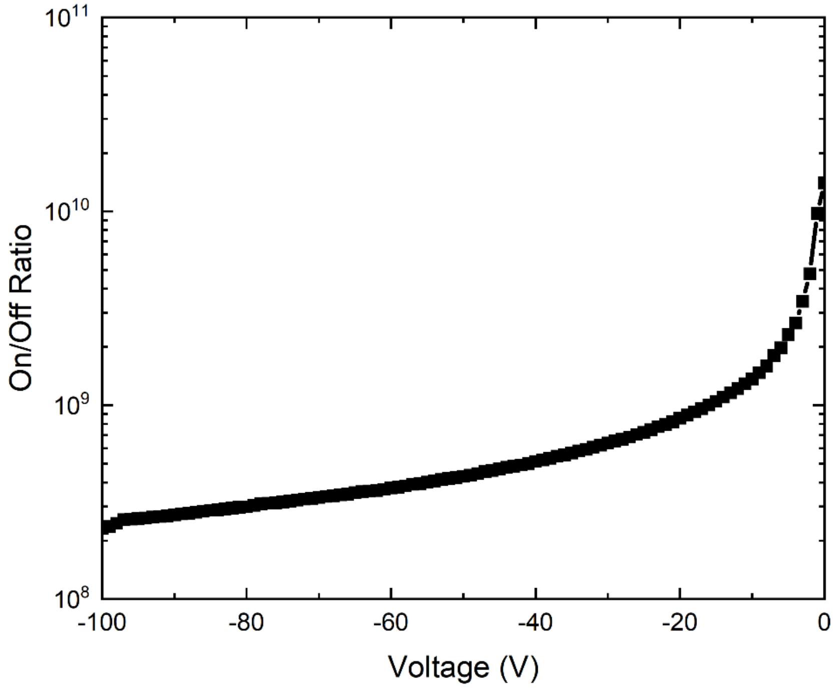

10^11
10^10
10^9
10^8
On/Off Ratio
-100
-80
-60
-40
-20
0
Voltage (V)

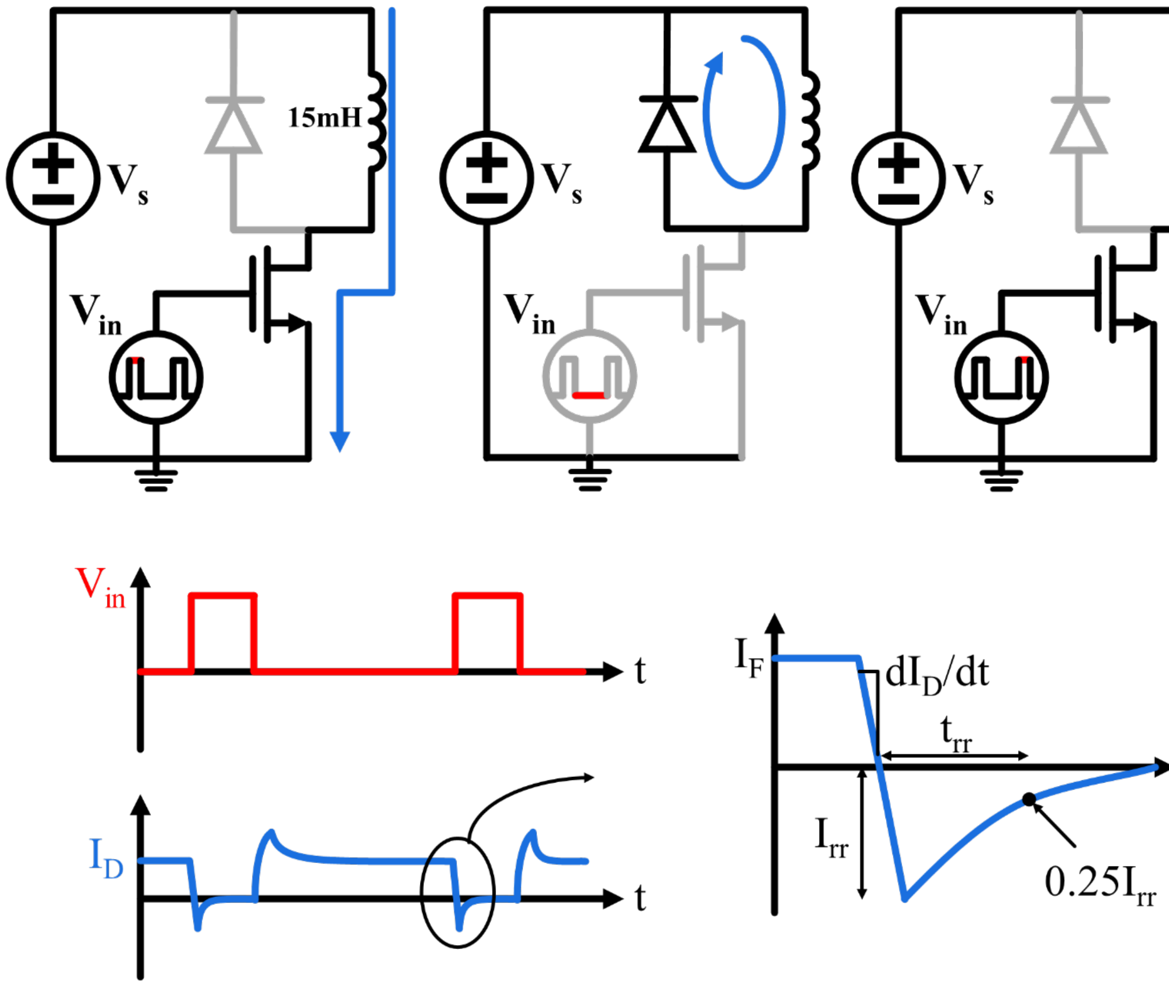
15mH
V$_s$
V$_{in}$
V$_s$
V$_{in}$
V$_s$
V$_{in}$
V$_{in}$
t
I$_D$
t
I$_F$
dI$_D$/dt
t$_{rr}$
I$_{rr}$
0.25I$_{rr}$

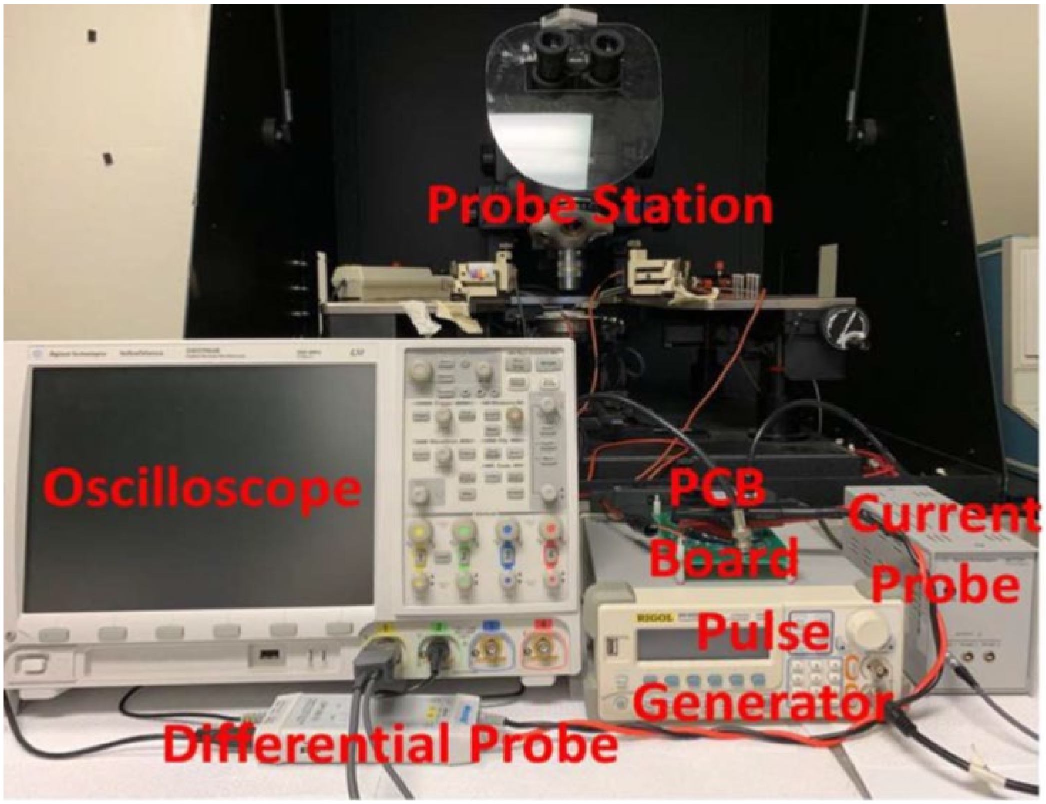
Probe Station
Oscilloscope
PCB Board
Current Probe
Pulse Generator
Differential Probe

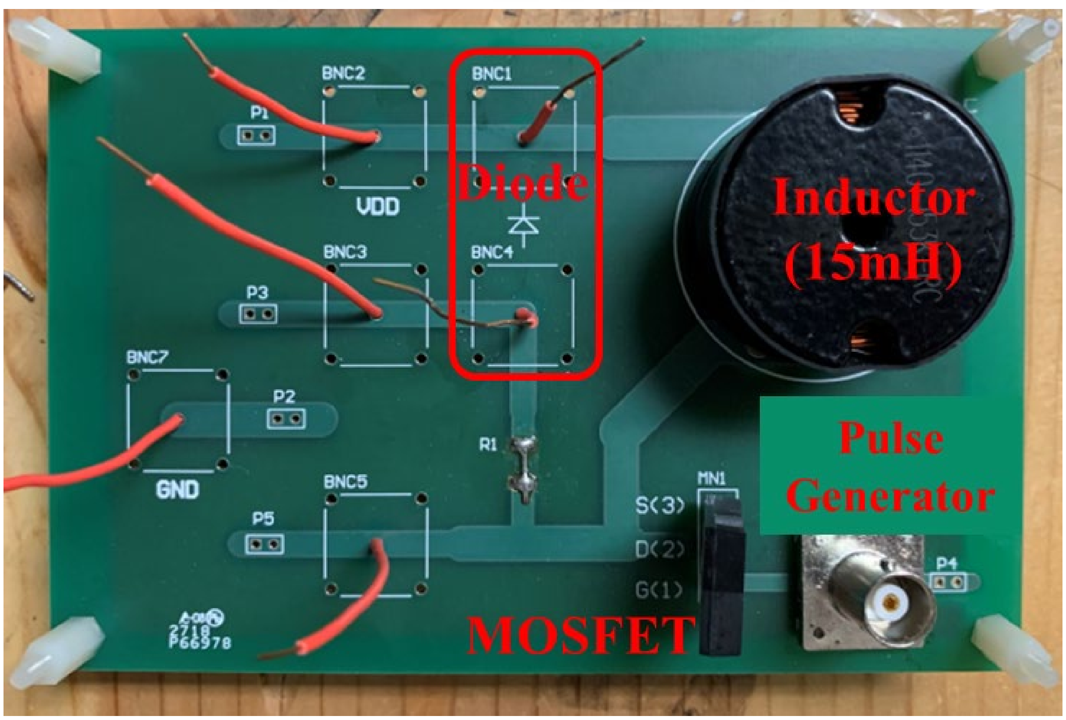
BNC2
BNC1
P1
VDD
Diode
Inductor (15mH)
BNC3
BNC4
P3
BNC7
P2
R1
GND
BNC5
P5
MN1
S(3)
D(2)
G(1)
Pulse Generator
P4
MOSFET

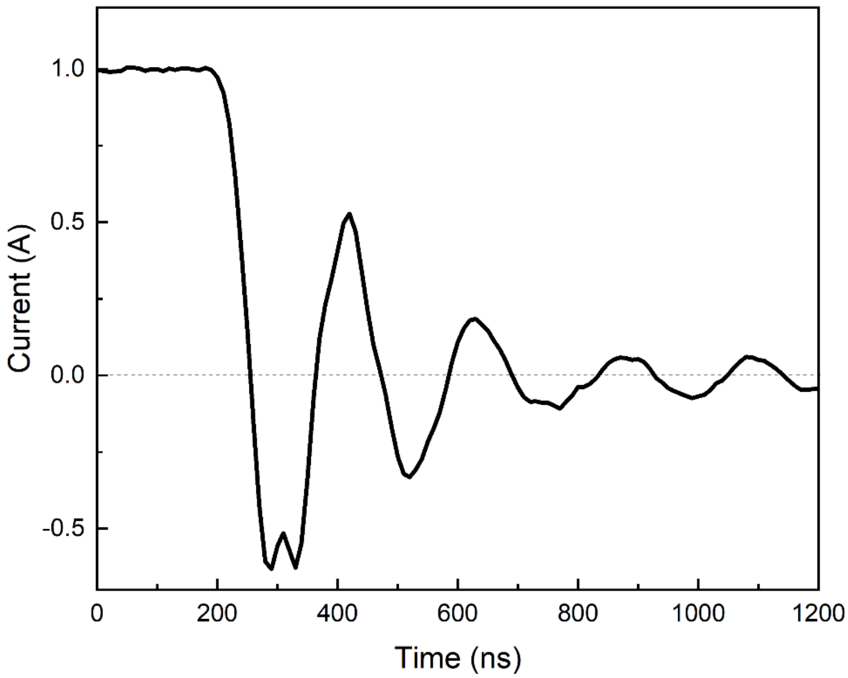
1.0
0.5
0.0
-0.5
Current (A)
0
200
400
600
800
1000
1200
Time (ns)